2952 *Biochemistry* **2010,** *49,* 2952–2961
DOI: 10.1021/bi902048c

BIOCHEMISTRY
including biophysical chemistry & molecular biology
*Article*

# Role of Valine 464 in the Flavin Oxidation Reaction Catalyzed by Choline Oxidase[†,‡]

Steffan Finnegan,[§] Johnson Agniswamy,[∥] Irene T. Weber,[§,⊥,∥] and Giovanni Gadda*[,§,∥,⊥]

[§]*Departments of Chemistry,* [∥]*Biology, and* [⊥]*The Center for Biotechnology and Drug Design, Georgia State University, Atlanta, Georgia 30302-4098*

*Received December 1, 2009; Revised Manuscript Received February 10, 2010*

ABSTRACT: The oxidation of reduced flavin cofactors by oxygen is a very important reaction that is central to the chemical versatility of hundreds of flavoproteins classified as monooxygenases and oxidases. These enzymes are characterized by bimolecular rate constants $\geq 10^5$ $M^{-1}$ $s^{-1}$ and produce water and hydrogen peroxide, respectively. A hydrophobic cavity close to the reactive flavin C(4a) atom has been previously identified in the 3D structure of monooxygenases but not in flavoprotein oxidases. In the present study, we have investigated by X-ray crystallography, mutagenesis, steady-state, and rapid reaction approaches the role of Val464, which is $< 6$ Å from the flavin C(4a) atom in choline oxidase. The 3D structure of the Val464Ala enzyme was essentially identical to that of the wild-type enzyme as shown by X-ray crystallography. Time-resolved anaerobic substrate reduction of the enzymes showed that replacement of Val464 with alanine or threonine did not affect the reductive half-reaction. Steady-state and rapid kinetics as well as enzyme-monitored turnovers indicated that the oxidative half-reaction in the Ala464 and Thr464 enzymes was decreased by ~50-fold with respect to the wild-type enzyme. We propose that the side chain of Val464 in choline oxidase provides a nonpolar site that is required to guide oxygen in proximity of the C(4a) atom of the flavin, where it will subsequently react via electrostatic catalysis. Visual analysis of available structures suggests that analogous nonpolar sites are likely present in most flavoprotein oxidases. Mechanistic considerations provide rationalization for the differences between sites in monooxygenases and oxidases.

The oxidation of reduced flavin cofactors by molecular oxygen, or the lack thereof, is a very important chemical reaction that is at the core of the chemical versatility displayed by flavoenzymes. Flavoenzymes comprise hundreds of enzymes catalyzing the most diverse biochemical reactions. Depending upon the ability to react with oxygen and the product of oxygen reduction, three general classes of flavoenzymes are distinguished (*1*, *2*). Flavoprotein dehydrogenases show very little or no reactivity with oxygen, thereby requiring other electron acceptors for catalytic turnover. On the other hand, monooxygenases and oxidases show high reactivity with oxygen, which is usually characterized by second-order rate constants $\geq 10^5$ $M^{-1}$ $s^{-1}$, with water and hydrogen peroxide being produced in the reactions, respectively (*1*). Reduced flavins existing free in solution, i.e., not associated with a protein, also reduce oxygen, but with much slower bimolecular rate constants around $2.5 \times 10^2$ $M^{-1}$ $s^{-1}$ (*3*). It is therefore the protein microenvironment surrounding the flavin in flavoprotein dehydrogenases, monooxygenases, and oxidases that modulates the extent to which the reduced flavin reacts with oxygen in these different classes of enzymes (*2*, *4*, *5*).

Several studies on a number of enzymes have contributed to the current knowledge of the features in the active sites of flavoenzymes that contribute to the up- and downmodulation of oxygen reactivity. A classical example of a dehydrogenase, where oxygen reactivity is suppressed due to ligand binding, is mammalian medium-chain acyl-CoA dehydrogenase, where the presence of the ligand has been shown to increase the redox potential of the flavin and to desolvate the active site (*6*, *7*). Lack of oxygen reactivity can also be due to steric effects arising from the presence of amino acid side chains that physically prevent oxygen from approaching the reactive C(4a) atom of the reduced flavin (see Scheme 1 for flavin numbering), as in the case of the alanine residues in the active sites of a mutant form of L-lactate monooxygenase (*8*) and L-galactono-$\gamma$-lactone dehydrogenase (*9*). On the other hand, studies on glucose oxidase using mechanistic and structural approaches have established that the presence of a positive charge on a histidine residue in proximity of the flavin C(4a) atom is required to stabilize the negatively charged superoxide species that is formed transiently in the reaction of the reduced flavin with oxygen (Scheme 1) (*10*−*13*). Similar activations of molecular oxygen have been proposed in monomeric sarcosine oxidase and choline oxidase, where the positive charge is provided by an active site lysine in the former and the trimethylammonium moiety of the enzyme-bound substrate in the latter (Scheme 1) (*14*−*16*). Based on a combination of site-directed mutagenesis with mechanistic and structural investigations, a hydrophobic tunnel has been proposed to guide oxygen to the C(4a) atom of the reduced flavin in cholesterol oxidase (*17*). More recently, an integrated approach based on X-ray crystallography, enhanced-statistics molecular dynamics simulations, kinetics, and site-directed mutagenesis allowed the authors to propose the presence of multiple diffusion pathways that converge to the reactive center on the flavin in the monooxygenase component $C_2$ of *p*-hydroxyphenylacetate hydroxylase and alditol oxidase (*18*). In this respect, the three-dimensional structure of the monooxygenase component $C_2$ of *p*-hydroxyphenylacetate hydroxylase also shows the presence of a hydrophobic cavity with

[†]This work was supported in part by grants from NSF-CAREER MCB-0545712 (G.G.) and an MBD Fellowship from Georgia State University (S.F.).

[‡]The atomic coordinates and structure factors have been deposited in the Protein Data Bank as entry 3LJP.

*Corresponding author. Phone: (404) 413-5537. Fax: (404) 413-5505. E-mail: ggadda@gsu.edu.

 Published on Web 02/25/2010 © 2010 American Chemical Society

Scheme 1: Activation of Oxygen by a Positively Charged Group in Glucose Oxidase, Monomeric Sarcosine Oxidase, and Choline Oxidase

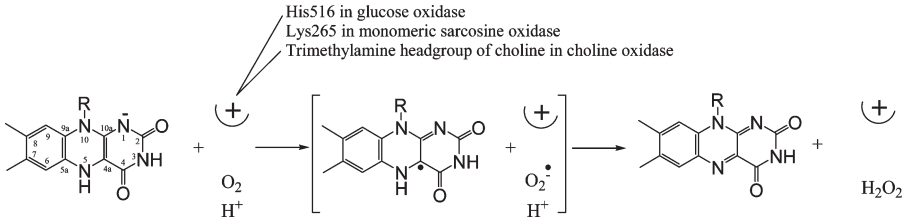


Scheme 2: Two-Step Oxidation of Choline Catalyzed by Choline Oxidase

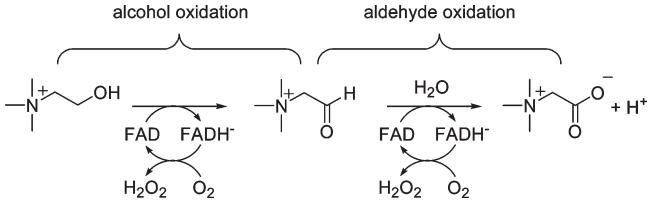


proper geometry in proximity of the C(4a) atom of the flavin, a feature that is not structurally apparent in flavoprotein oxidases (*19*). These results collectively present general principles for the reaction with oxygen or lack thereof in flavoproteins. They do not, however, directly address whether the site in flavoprotein oxidases where oxygen reacts with the reduced flavin has some nonpolar character in addition to the positively charged group that is required for the activation of oxygen (Scheme 1).

Our group has investigated the reaction of alcohol oxidation catalyzed by the FAD[1]-containing choline oxidase from *Arthrobacter globiformis* using biochemical (*20*−*23*), structural (*24*, *25*), site-directed mutagenic (*15*, *21*, *25*−*28*), and mechanistic (*29*−*35*) approaches. The enzyme catalyzes the two-step, flavin-linked oxidation of choline to glycine betaine, with betaine aldehyde as intermediate and molecular oxygen as electron acceptor (Scheme 2). A detailed mechanistic understanding of the reductive half-reaction where a hydride ion is transferred from choline to the enzyme-bound flavin has emerged from these studies (for a recent review see ref *36*). The subsequent oxidation of the enzyme-bound, reduced flavin with oxygen occurs while the active site is still occupied with the aldehyde intermediate of the reaction, as suggested by steady-state kinetic studies with choline and a number of substrate analogues (*15*, *16*, *23*, *31*, *34*). In this respect, site-directed mutagenesis studies where each of the three histidine residues located in the active site of the enzyme were individually replaced indicated that these residues do not contribute to oxygen activation, as the bimolecular rate constants for oxygen reaction ($k_{cat}/K_{oxygen}$) were not significantly altered in the mutant enzymes from the value of $\sim 10^5$ $M^{-1}$ $s^{-1}$ of the wild-type enzyme (*27*, *37*, *38*). In contrast, substitution of the positively charged substrate with the isosteric analogue devoid of charge 3,3-dimethylbutan-1-ol yielded $k_{cat}/K_{oxygen}$ values of $\sim 10^3$ $M^{-1}$ $s^{-1}$, consistent with activation of oxygen for reaction with the reduced flavin being exerted by the enzyme-bound ligand (*15*, *16*). In agreement with this conclusion, the His99Asn, His351Ala, His466Ala, and wild-type forms of choline oxidase showed $k_{cat}/K_{oxygen}$ values that are independent of pH, since the trimethylammonium moiety of the substrate cannot ionize (*15*, *23*, *27*, *32*, *37*, *38*). In the X-ray

[1]Abbreviations: DMB, 3,3-dimethylbutan-1-ol; FAD, flavin adenine dinucleotide; TMA, trimethylamine.

Scheme 3: Minimal Kinetic Mechanism for Reductive Half-Reaction of the Val464Ala and Val464Thr Enzymes[a]

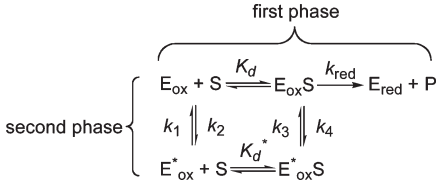


[a]$E_{ox}$, catalytically competent oxidized enzyme; $E_{ox}$*, catalytically incompetent enzyme; S, choline; $E_{red}$, reduced enzyme.

structure of choline oxidase previously solved to a resolution of 1.86 Å (*24*, *25*), Val464 lies in the active site cavity close to the C(4a)-N(5) atoms of the flavin, with its hydrophobic side chain in van der Waals contact with the C(2) atom of the conserved His466. Replacement of Val464 with threonine or alanine results in the ensuing variant enzymes having a catalytically incompetent form of enzyme in equilibrium with a competent form (Scheme 3) that is able to efficiently oxidize choline with rates similar to those determined for the wild-type enzyme (*28*).

In the present study, we have used X-ray crystallography, site-directed mutagenesis, and both steady-state and rapid kinetic approaches to investigate the role of the hydrophobic residue Val464 in the active site of choline oxidase. The three-dimensional structure of the Val464Ala enzyme was solved by X-ray crystallography to a resolution of 2.2 Å, and the oxidative half-reactions, steady-state kinetic mechanisms, and enzyme-monitored turnovers were investigated for the Val464Ala and Val464Thr variants along with the wild-type enzyme for comparison. Moreover, pH profiles of the $k_{cat}/K_{oxygen}$ values with choline as substrate and the effect of substituting choline with 3,3-dimethylbutan-1-ol on the $k_{cat}/K_{oxygen}$ values were investigated in the Val464Ala enzyme. The results presented established the hydrophobic side chain of Val464 as being important in the oxidative half-reaction of choline oxidase, with minimal effects on the reaction of choline oxidation and, most importantly, the three-dimensional structure of the enzyme. A role is proposed for Val464 in the flavin oxidation reaction catalyzed by choline oxidase. Analysis of the three-dimensional structures of several flavoprotein oxidases suggests that hydrophobic residues in the active site of these enzymes may have roles similar to that of Val464 in choline oxidase in the reaction of the reduced flavin with oxygen.

## EXPERIMENTAL PROCEDURES

*Materials*. *Escherichia coli* strain Rosetta(DE3)pLysS was from Novagen (Madison, WI). DNase was from Roche (Indianapolis, IN). The QuikChange site-directed mutagenesis kit was from Stratagene (La Jolla, CA). The QIAprep Spin

Miniprep kit was from Qiagen (Valencia, CA). Oligonucleotides used for sequencing of the mutant genes were custom synthesized by Sigma Genosys (Woodland, TX). Choline chloride was from ICN Pharmaceutical Inc. (Irvine, CA). 3,3-Dimethylbutan-1-ol (DMB), glucose, glucose oxidase, and betaine aldehyde were from Sigma (St. Louis, MO). All other reagents were of the highest purity commercially available.

*Site-Directed Mutagenesis*. The Val464Ala, Val464Thr, and Val464Leu enzymes were prepared using the pET/*codA* plasmid harboring the wild-type gene for choline oxidase as template for site-directed mutagenesis as previously described, and the presence of the desired mutation was confirmed by sequencing as described (*21*, *22*, *25*, *28*).

*Enzyme Expression and Purification*. The Val464Ala, Val464Thr, and wild-type enzymes were expressed and purified to homogeneity using the procedure described previously for the purification of the wild-type enzyme (*16*, *22*). Attempts to purify the Val464Leu enzyme were unsuccessful; stable and active enzyme could not be obtained due to protein instability during protein purification, thereby preventing the characterization of the Val → Leu substitution at position 464.

*Crystallization, X-ray Data Collection, and Refinement of the Val464Ala Enzyme*. Crystals of the Val464Ala enzyme were grown aerobically at room temperature by hanging drop vapor diffusion from 10% to 15% (v/v) polyethylene glycol MW 6000, 50−200 mM magnesium acetate, and 200 mM trimethylamine in 0.08 M sodium cacodylate, pH 6.0. Single crystals were transferred from the mother liquor into a cryoprotectant consisting of mother liquor with 25% (v/v) glycerol and allowed to soak for approximately 2 min prior to flash-freezing in liquid nitrogen. Diffraction data were collected at 100 K on beamline 22-ID of the Southeast Regional Collaborative Access Team (SER-CAT) at the Advanced Photon Source, Argonne National Laboratory. The data were integrated and scaled with HKL2000 (*39*).

The crystal structure of the Val464Ala enzyme was solved by molecular replacement using PHASER (*40*) in the CCP4i suite of programs using as the starting model the structure of wild-type choline oxidase (PDB code 2JBV) (*25*). The structure was subjected to several rounds of refinement in REFMAC (*41*) of CCP4. The molecular graphics programs O 9.0 (*42*) and Coot 0.33 (*43*) were used in model rebuilding. The solvent molecules were inserted at stereochemically reasonable positions based on the peak height of the $2F_o - F_c$ and $F_o - F_c$ electron density maps, hydrogen bond interactions, and interatomic distances. The geometry of the refined structures was validated according to the Ramachandran plot criteria (*44*). Molecular figures were prepared with MOLSCRIPT, RASTER3D (*45*) and PyMol (http://www.pymol.org).

*Enzyme-Monitored Turnover*. Enzyme-monitored turnover experiments were carried out by monitoring the absorbance at 455 nm as a function of time using an SF-61DX2 HI-TECH KinetAsyst high-performance stopped-flow spectrophotometer thermostated at 25 °C. The aerobic enzyme solution was mixed with an aerobic solution of 20 mM choline, both prepared in 50 mM sodium pyrophosphate, pH 10.0. The final [oxygen] was 0.25 mM; the final [choline] was 10 mM.

*Enzyme Kinetics*. Steady-state kinetic measurements were carried out by using the method of initial rates using a computer-interfaced Oxy-32 oxygen-monitoring system (Hansatech Instrument Ltd.) (*46*). The pH dependence of the bimolecular rate constants for reaction of the reduced flavin with oxygen ($k_{cat}/K_{oxygen}$) was determined by measuring enzymatic activity at varying concentrations of choline and oxygen in the pH range between 5.0 and 10.0 in 50 mM sodium pyrophosphate at 25 °C, with the exception of pH 7.0 where sodium phosphate was used. The assay reaction mixture was equilibrated at the desired oxygen concentration by bubbling with an $O_2/N_2$ gas mixture for at least 10 min before the reaction was started with the addition of the enzyme.

Oxidative half-reaction measurements for the wild-type, Val464Ala, and Val464Thr enzymes were carried out using an SF-61DX2 HI-TECH KinetAsyst high-performance stopped-flow spectrophotometer thermostated at 25 °C in 50 mM sodium pyrophosphate buffer, pH 10.0. The rate constants for flavin oxidation were measured by monitoring the increase in absorbance at 455 nm that results from the mixing of anaerobic reduced enzyme in 50 mM buffer with 50 mM buffer which was equilibrated at varying oxygen concentrations by sparging with an $O_2/N_2$ gas mixture for at least 10 min prior to mixing. The enzymes were previously reduced by anaerobic mixing of the oxidized enzymes with a 1.1 molar excess of betaine aldehyde.

*Data Analysis*. Kinetic data were fit with KaleidaGraph (Synergy Software, Reading, PA) or the Kinetic Studio Software Suite (Hi-Tech Scientific, Bradford on Avon, U.K.). A first attempt at the determination of the steady-state kinetic parameters for the Val464Ala and Val464Thr enzymes at varying concentrations of both choline and oxygen was carried out by fitting the initial rates to eq 1, which describes a steady-state kinetic mechanism with formation of a ternary complex. $K_{choline}$ and $K_{oxygen}$ are the Michaelis constants for choline and oxygen, respectively, and $k_{cat}$ is the true turnover number of the enzyme ($e$) at saturating concentrations of both choline and oxygen. This approach yielded estimated $K_{oxygen}$ values in the 5−8 mM range, which were ≥5-fold higher than the highest concentration of oxygen that was used in the experiments, thereby preventing saturation of the enzyme with oxygen. Thus, the true value for $k_{cat}$, as well as the derivative parameter $k_{cat}/K_{oxygen}$, could not be determined by using eq 1. Since the $k_{cat}/K_{oxygen}$ value represents the bimolecular rate constant for the capture of oxygen onto the enzyme when [oxygen] < $K_{oxygen}$, it could be determined graphically as described below (eq 2). Here, the $k_{cat}/K_{oxygen}$ values were determined from the reciprocal of the $y$-intercept of a secondary plot of the slopes of the lines obtained from the primary double reciprocal plot of $e/v_o$ versus 1/[oxygen] (i.e., $\text{slope}_{1/[oxygen]}$) as a function of 1/[choline] (*47*):

$$\frac{v}{e} = \frac{k_{cat}[\text{choline}][\text{oxygen}]}{K_{choline}[\text{oxygen}] + K_{oxygen}[\text{choline}] + [\text{choline}][\text{oxygen}] + K_{ia}K_{oxygen}} \quad (1)$$

$$\text{slope}_{1/[oxygen]} = \frac{K_{oxygen}}{k_{cat}} + \left(\frac{K_{iA}K_{oxygen}}{k_{cat}}\right)\frac{1}{[\text{choline}]} \quad (2)$$

Stopped-flow traces for the oxidative half-reaction were fit with eq 3, which describes a single-exponential process in which $k_{obs}$ is the observed rate constant for the increase in absorbance at 455 nm, $A$ is the absorbance at time $t$, $B$ is the amplitude of the absorbance change, and $C$ is an offset value that accounts for the nonzero absorbance value at infinite time.

$$A = B\exp(-k_{obs}t) + C \quad (3)$$

The pre-steady-state bimolecular rate constant for flavin oxidation was determined with eq 4. Here, the $k_{obs}$ value is the

observed rate constant associated with flavin oxidation at any given concentration of oxygen, and $k_{ox}$ is the second-order rate constant for flavin oxidation.

$$k_{obs} = k_{ox}[\text{oxygen}] \quad (4)$$

## RESULTS

*Determination of the Crystal Structure of the Val464Ala Enzyme*. The Val464Ala enzyme was crystallized in the tetragonal space group $P4_32_12$ with a homodimer in the asymmetric unit. The structure was refined to the resolution of 2.2 Å and *R*-factor of 16.5%. The X-ray diffraction data and refinement statistics are listed in Table 1. Although the replacement of the side chain of residue 464 from valine to alanine results in loss of van der Waals interactions between Ala464 and His310, Glu312, His351, and Asn378, these residues are located in the same position in the mutant and wild-type enzymes (2JBV) (Figure 1). The homodimers of the Val464Ala enzyme could be superimposed with those of the wild-type enzyme with an rmsd value of 0.67 Å for 1056 topologically equivalent Cα atoms, consistent with the overall structure of the Val464Ala enzyme being essentially identical to that of the wild-type choline oxidase (2JBV) previously reported. The individual monomers of the Val464Ala enzyme are even more similar to those of the wild-type choline oxidase with rmsd values of 0.29 and 0.25 Å for the A and B chain, respectively. Furthermore, the two monomers within the structure of the Val464Ala enzyme are very similar to one another, as evident from the rmsd values of 0.22 for 528 common Cα atoms.

The FAD in the Val464Ala enzyme is covalently bound to the Nε2 atom of His99 as in the case of wild-type (*25*). The $2F_o - F_c$ electron density map of FAD contoured at 1σ is shown in Figure 1. A striking difference between the structures of the Val464Ala and wild-type enzymes is the absence of the C(4a) oxygen adduct on the *re*-face of the FAD cofactor, observed in the wild-type enzyme, on the FAD cofactor in the Val464Ala variant enzyme, resulting in the isoalloxazine moiety of the FAD cofactor in the variant enzyme being more planar than that in the wild-type (Figure 1b). This difference is consistent with the C(4a) atom of the of the FAD cofactor being $sp^3$ hybridized in the wild-type enzyme due to the presence of the C(4a) adduct as compared to $sp^2$ hybridized in the Val464Ala enzyme. For the wild-type choline oxidase the enzyme-bound FAD is likely reduced in the X-ray beam during data collection, and the reduced FAD then forms either a C(4a)-OH or C(4a)-OO(H) adduct but an insufficient proton inventory prevents the FAD reoxidation to proceed (*24*). The absence of the FAD C(4a) adduct in the crystal structure of the Val464Ala enzyme is most likely due to the lowered apparent affinity for oxygen in the Val464Ala variant enzyme as compared to the wild-type enzyme as observed by the inability to saturate the Val464Ala enzyme with oxygen in the steady-state kinetic studies. Alternatively, it may simply be due to the FAD not being reduced during the data collection and thus making the formation of the C(4a) adduct impossible in the synchotron. The crystallization conditions for both the wild-type and the variant enzyme do not contain any reagents known to form C(4a) adducts with FAD.

Overall, with the exception of the point mutation that replaces Val464 with alanine, the orientation and position of all the amino acid residues in the active site and in the vicinity of the Ala464 position in the Val464Ala enzyme are closely identical to those of the wild-type form of choline oxidase, as illustrated in Figure 1.

Table 1: Crystallographic Data Collection and Refinement Statistics

| | choline oxidase Val464Ala |
|---|---|
| space group | $P4_32_12$ |
| $a = b$ (Å) | 87.04 |
| $c$ (Å) | 353.07 |
| resolution range | 50−2.2 |
| total observations | 411516 |
| unique reflections | 67756 |
| completeness | 96.0 (99.5)[a] |
| $\langle I/\sigma(I)\rangle$ | 12.3 (5.5) |
| $R_{sym}$ (%)[b] | 13.4 (37.6) |
| resolution range | 50−2.2 |
| $R_{cryst}$ (%)[c] | 16.5 |
| $R_{free}$ (%)[d] | 22.7 |
| mean *B*-factor (Å$^2$) | 19.4 |
| number of atoms | |
| protein | 8302 |
| FAD | 106 |
| water | 472 |
| rms deviations | |
| bond length (Å) | 0.025 |
| angle (deg) | 2.08 |

[a]Values in parentheses are given for the highest resolution shell. [b]$R_{sym} = \sum_{hkl}|I_{hkl} - \langle I_{hkl}\rangle|/\sum_{hkl}I_{hkl}$. [c]$R = \sum|F_o - F_c|/\sum F_o$. [d]$R_{free} = \sum_{test}(|F_o| - |F_c|)^2/\sum_{test}|F_o|^2$.

The point mutation at position 464 results in an important difference observable in the structures of the Val464Ala variant and the wild-type enzyme, which is a significant increase in the size of the pocket on the *re*-face directly above the C(4a)-N(5) atoms of the flavin. This pocket is defined by His351, Ala464, and His466 and is the location where the C(4a) oxygen adduct is observed in the crystal structure of the wild-type enzyme, consistent with this being the site of oxygen reduction. In this regard, a 2 Å increase is seen in the distance between the C(4a)-N(5) atoms of FAD and the nearest side chain atom CB of Ala464 with respect to the distance to side chain atom CG1 of Val464 in the wild-type enzyme.

Interestingly, only one form of the Val464Ala variant enzyme is observable in the crystal structure solved even though the enzyme has previously been shown to exist in an equilibrium between an incompetent and a competent form (*28*). The crystallization conditions for Val464Ala included 200 mM trimethylamine, which is a substrate analogue known to be a competitive inhibitor of the wild-type choline oxidase (*16*). Although trimethylamine is not observed in the 3D X-ray crystal structure of the enzyme, it may have contributed to the selective crystallization of only one form of the Val464Ala variant enzyme. Alternatively, the $\Delta H_{fusion}$ for the phase change associated with the crystallization may be sufficient to shift the equilibrium during this process to a point where the crystal only contains one form of enzyme.

*Steady-State Kinetic Mechanism of Val464Ala and Val464Thr Enzymes*. The steady-state kinetic mechanisms of the Val464Ala and Val464Thr enzymes were investigated with the method of the initial rates by monitoring the rates of oxygen consumption in a Clark oxygen electrode in the pH range from 5.0 to 10.0 at varying concentrations of both choline and oxygen. The analysis of the collected data is shown here exemplified by the data collected at pH 8.0 and 25 °C. With both enzymes, a double reciprocal plot of the initial rates of reaction as a function of [choline] yielded intersecting lines, as previously reported for the wild-type and several mutants of choline oxidase (*25*, *27*, *37*, *38*, *48*−*50*).

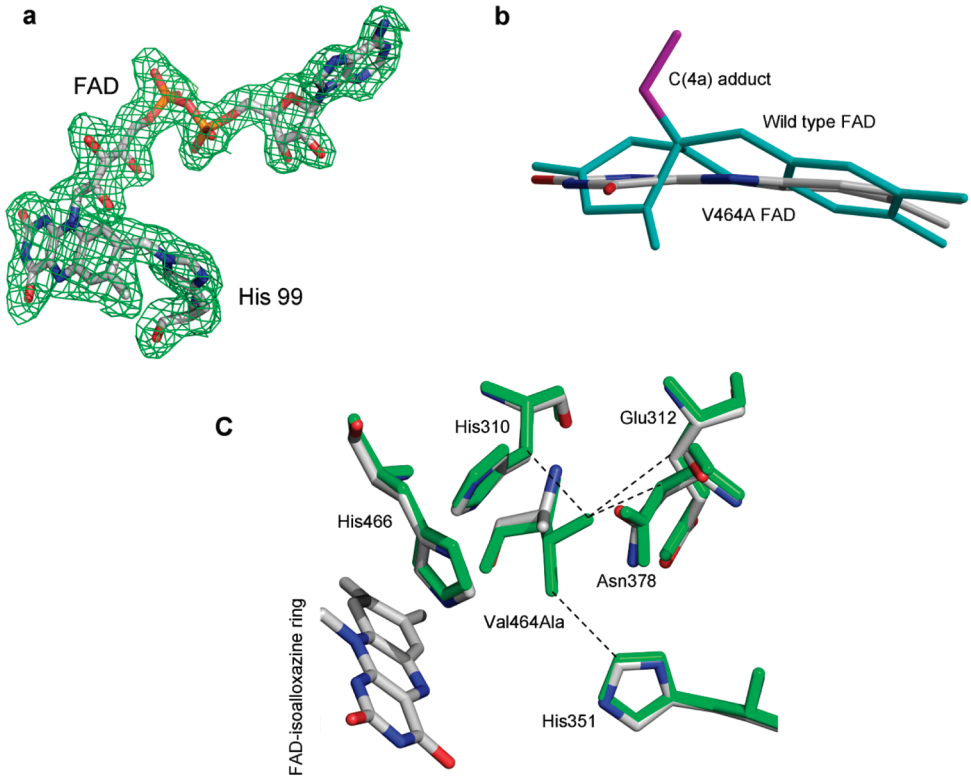


FIGURE 1: Crystal structure of the Val464Ala mutant. Panel a shows the $2F_o - F_c$ electron density map of FAD contoured at a level of $1\sigma$. The FAD is covalently bound to His99. Panel b illustrates the superposition of the FAD isoalloxazine ring from the wild-type (cyan) and the Val464Ala enzymes (colored by element type) of choline oxidase. The C(4a) oxygen adduct of wild-type FAD is shown in magenta. Note that the isoalloxazine ring of the Val464Ala enzyme is more planar than that of the wild-type structure. Panel c shows the Val464Ala mutation site. The van der Waals interactions between the side chains of Val464 (green) and residues His310, Glu312, His351, and Asn378, indicated by broken lines, are lost in the structure of the Val464Ala enzyme. Despite the loss of these interactions, these residues in the Val464Ala enzyme maintain virtually identical conformations and positions to those in the wild-type enzyme.

Therefore, the $k_{cat}/K_{oxygen}$ value is not independent of the concentration of choline, unless oxygen is saturating (*47*). The data with the Val464Ala enzyme were fit well with eq 1, yielding, however, computer-estimated $K_{oxygen}$ values in the 5−8 mM range, which was at least 5-fold larger than the highest [oxygen] used (i.e., 1 mM). Lack of enzyme saturation with oxygen thereby prevented the use of eq 1 for the determination of the steady-state kinetic parameters of the enzyme. The $k_{cat}/K_{oxygen}$ values were therefore determined graphically with the data at hand by using eq 2, as described in the Experimental Procedures. This yielded a $k_{cat}/K_{oxygen}$ value of $1500 \pm 150$ $M^{-1}$ $s^{-1}$ at pH 8.0.

With the Val464Thr enzyme, the dependences of the initial rates of reaction on [oxygen] at different concentrations of choline showed sigmoidal rather than hyperbolic patterns (Figure 2) and were fit best to a Hill equation. As for the case of the Val464Ala enzyme, the estimated $K_{oxygen}$ values were well above the maximal [oxygen] of ~1 mM that was used, thereby precluding the determination of meaningful kinetic parameters. Moreover, the sigmoidal kinetic patterns prevented the determination of the $k_{cat}/K_{oxygen}$ values for the Val464Thr enzyme by using the graphical methods employed for the Val464Ala enzyme. A kinetic behavior similar to that shown by the Val464Thr enzyme was recently reported for selected active site variants of cholesterol oxidase, where the observations were explained with a rate-limiting interconversion of multiple forms of enzyme reacting differently with oxygen (*17*). Although this interpretation could satisfactorily explain the steady-state kinetic pattern of the Val464Thr enzyme, lack of saturation of the enzyme with oxygen did not allow us to further investigate the steady-state kinetic

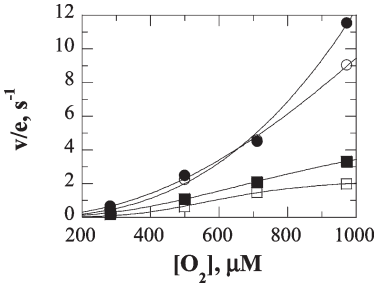


FIGURE 2: Dependence of the initial rates of reaction with choline as substrate for the Val464Thr enzyme as a function of [oxygen] in 50 mM sodium pyrophosphate, pH 10.0 and 25 °C. Choline concentrations were 5 mM (●), 1 mM (○), 0.1 mM (■), and 0.05 mM (□). The curves are independent fits of the data to the Hill equation ($v/e = k_{cat}[\text{oxygen}]^h/(K_{oxygen}{}^h + [\text{oxygen}]^h)$).

mechanism and draw conclusions on the steady-state behavior of the Val464Thr enzyme.

*pH Dependence of the $k_{cat}/K_{oxygen}$ Values of the Val464Ala Enzyme*. The effect of pH on the $k_{cat}/K_{oxygen}$ values of the Val464Ala enzyme is shown in Figure 3. As for the case of the wild-type enzyme (*32*), the Val464Ala enzyme had $k_{cat}/K_{oxygen}$ values that were independent of the pH between 5.0 and 10.0, however with an average value of $1700 \pm 150$ $M^{-1}$ $s^{-1}$. This value is ~50-fold lower than the pH-independent $k_{cat}/K_{oxygen}$ value of 90000 $M^{-1}$ $s^{-1}$ that was previously reported for the wild-type enzyme (*32*), indicating that the oxidative half-reaction in choline oxidase is affected substantially by the replacement of Val464 with alanine.

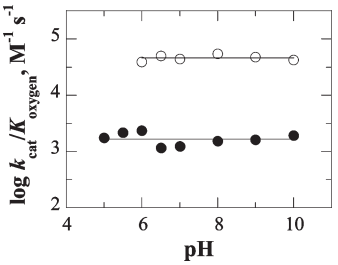


FIGURE 3: Effect of pH on the $k_{cat}/K_{oxygen}$ values with choline as substrate for the Val464Ala enzyme (●) compared to wild-type enzyme (○). The lines that fit the $k_{cat}/K_{oxygen}$ values represent the average of the values. Data for the wild-type enzyme are from ref *32*.

*Oxidative Half-Reactions of Wild-Type, Val464Ala, and Val464Thr Enzymes at pH 10.0*. The oxidative half-reactions where the reduced Val464Ala, Val464Thr, and the wild-type enzymes were oxidized with oxygen were investigated using a stopped-flow spectrophotometer. The rate constants for flavin oxidation were measured from the increase in absorbance at 455 nm of the flavin cofactor at various concentrations of oxygen at pH 10.0 and 25 °C. As shown in Figure 4, for all three investigated enzymes the oxidation of the flavin from the hydroquinone to the fully oxidized state was monophasic, without formation of any detectable transient species. The monophasic behavior of FAD oxidation in the Val464 variant enzymes is consistent with the mechanism shown in Scheme 3, showing that upon complete reduction of the FAD cofactor by the substrate only one form of reduced enzyme is present. With all investigated enzymes, the observed rate constants for flavin oxidation ($k_{obs}$) when plotted as a function of the concentration of oxygen defined second-order processes (Figure 4). For the wild-type enzyme the $k_{ox}$ was 1900 ± 40 $M^{-1}$ $s^{-1}$, whereas for the Val464Ala and Val464Thr enzymes it was 100 ± 2 $M^{-1}$ $s^{-1}$ and 125 ± 4 $M^{-1}$ $s^{-1}$, respectively. These $k_{ox}$ values refer to the free enzymes and therefore do not reflect the values that would be measured in enzymatic turnover where oxygen reacts with the reduced flavin when the active site is occupied with the product of the oxidation reaction; however, they demonstrate that the Val464Ala and Val464Thr enzymes are impaired to similar extents in their ability to react with oxygen with respect to the wild-type enzyme, with a significant decrease in the $k_{ox}$ values. Attempts to determine the $k_{ox}$ values for the three enzymes with the substrate bound were unsuccessful, due to the inability to obtain a stable reduced enzyme−substrate complex.

*Enzyme-Monitored Turnover of Val464Ala, Val464Thr, and Wild-type Enzymes*. Enzyme-monitored turnovers were carried out on the Val464Ala and Val464Thr enzymes under atmospheric oxygen conditions (i.e., 0.25 mM oxygen) with 10 mM choline at pH 10.0 in a stopped-flow spectrophotometer. As shown in Figure 5, the enzymes reached steady-state conditions of turnover with choline and oxygen when the absorbance at 455 nm was about two-thirds that of the fully oxidized, resting enzymes. This value corresponded well with the fraction of enzyme that is present in the catalytically competent form (i.e., 65%), which was previously determined for both the Val464Ala and Val464Thr enzymes (*28*). Since complete conversion of the incompetent to competent forms of the Val464 variant enzymes occurs over several seconds (*28*), during the steady-state catalytic turnover of Figure 5 the majority of the enzyme-bound flavin was in the reduced form in the Val464Ala and Val464Thr enzymes that are competent for catalysis. The reductive half-reaction in

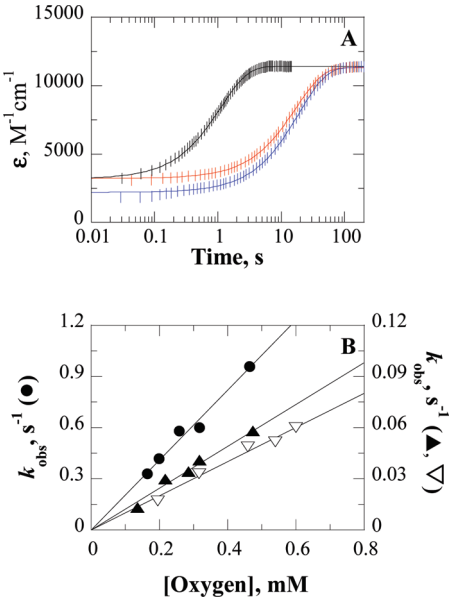


FIGURE 4: Time-resolved, flavin oxidation of the Val464Ala, Val-464Thr, and wild-type enzymes with oxygen in 50 mM sodium pyrophosphate, pH 10.0 and 25 °C, monitored at 455 nm in a stopped-flow spectrophotometer. Panel A shows the oxidation traces of the wild-type enzyme with 460 μM oxygen (black), Val464Thr with 475 μM oxygen (red), and Val464Ala with 460 μM oxygen (blue). All traces were fit to eq 3, yielding $R^2$ values > 0.999. For clarity, only one experimental point out of every two points is shown for the wild-type enzyme (vertical lines), and one out of ten points is shown for both Val464Ala and Val464Thr. The time indicated is after the end of flow, i.e., 2.2 ms. Panel B shows the dependence of the observed rate constants for flavin oxidation as a function of the concentration of oxygen for the wild-type (●), Val464Ala (▽), and Val464Thr (▲) enzymes. For each enzyme the observed rate constants were fit to eq 4.

both the Val464-substituted enzymes is minimally affected with respect to the wild-type enzyme (*28*), and the two enzymes also show similar behavior in the enzyme-monitored turnover. Hence, it can be concluded that the oxidative half-reactions are affected to similar extents in the Val464Ala and Val464Thr enzymes with respect to the wild-type choline oxidase. In this respect, a control experiment with the wild-type enzyme showed that ~20% of the enzyme-bound flavin is in the oxidized state under catalytic turnover of the enzyme in the same conditions (Figure 5), consistent with the much higher bimolecular rate constant $k_{cat}/K_{oxygen}$ for the oxidative half-reaction of the wild-type enzyme (*32*).

*$k_{cat}/K_{oxygen}$ Values of the Val464Ala Enzyme with 3,3-Dimethylbutan-1-ol as Substrate*. The $k_{cat}/K_{oxygen}$ values of the Val464Ala enzyme were also determined with 3,3-dimethylbutan-1-ol, an isosteric analogue of choline that contains a *tert*-butyl headgroup devoid of charge. The effect of the substrate analogue on $k_{cat}/K_{oxygen}$ for the Val464Ala enzyme was determined at pH 8.0 in order for it to be directly compared to a previous study performed on the wild-type enzyme (*16*). As for the case of choline as substrate, the Val464Ala enzyme could not be saturated with oxygen due to $K_{oxygen}$ being significantly larger than the highest [oxygen] of ~1 mM that was attainable in the experiment (data not shown). Consequently, the apparent $k_{cat}/K_{oxygen}$ values were determined by measuring initial rates of reaction as a function of [oxygen] at fixed saturating concentrations of 3,3-dimethylbutan-1-ol. As shown in Table 2, similar $^{app}(k_{cat}/K_{oxygen})$ values were determined with 10, 30, and 40 mM

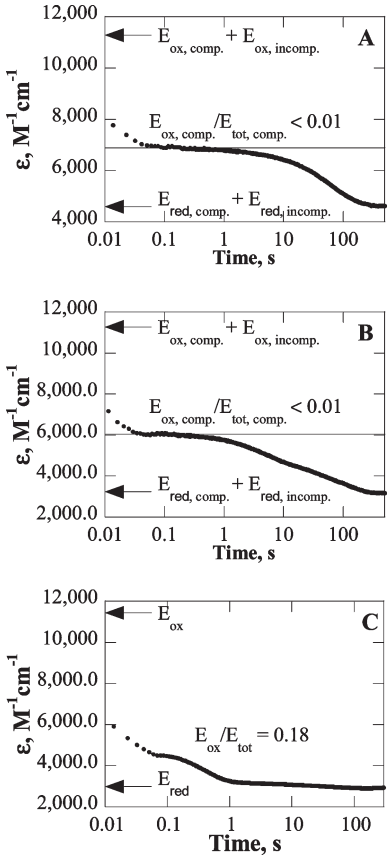


FIGURE 5: Enzyme-monitored turnovers with choline and oxygen as substrates for the Val464Ala (panel A), Val464Thr (panel B), and wild-type (panel C) enzymes. In all cases, [choline] = 10 mM, [oxygen] = 0.25 mM, pH 10.0 and 25 °C. The top arrow corresponds to the extinction coefficient at 455 nm of the fully oxidized enzyme (both the catalytically competent and incompetent forms for the Val464-substituted enzymes), while the bottom arrow corresponds to the fully reduced enzyme after oxygen depletion in the reaction mixture (and also full conversion of the incompetent to catalytically competent forms for the Val464 substituted enzymes). The horizontal lines in panels A and B define the expected absorbance during turnover of the Val464Ala and Val464Thr enzyme when all of the catalytically competent form of the enzyme is in the reduced state and the incompetent form of the enzyme, which does not undergo turnover, is still present in the oxidized form before slowly converting to the catalytically competent form. The ratios $E_{ox}/E_{tot}$ are estimations of the fraction of oxidized (catalytically competent) enzyme with respect to the total enzyme that is catalytically competent for turnover.

Table 2: $^{app}(k_{cat}/K_{oxygen})$ for the Val464Ala Enzyme at Fixed Saturating Concentrations of 3,3-Dimethylbutan-1-ol as Substrate [a]

| [3,3-dimethylbutan-1-ol], mM | $^{app}(k_{cat}/K_{oxygen})$, $M^{-1}$ $s^{-1}$ |
|---|---|
| 10 | 33 ± 1 |
| 30 | 30 ± 1 |
| 40 | 31 ± 1 |

[a] Conditions: 50 mM sodium pyrophosphate, 25 °C, pH 8.0.

3,3-dimethylbutan-1-ol, establishing a true $k_{cat}/K_{oxygen}$ value of 31 ± 2 $M^{-1}$ $s^{-1}$ at pH 8.0 for the reaction of the Val464Ala enzyme with 3,3-dimethylbutan-1-ol as substrate. Thus, the lack of positive charge on the organic substrate bound at the active site of the enzyme results in a further decrease of ~55-fold in the $k_{cat}/K_{oxygen}$ value of the Val464Ala enzyme (i.e., 1700 $M^{-1}$ $s^{-1}$ with choline as substrate). For comparison, a similar decrease of

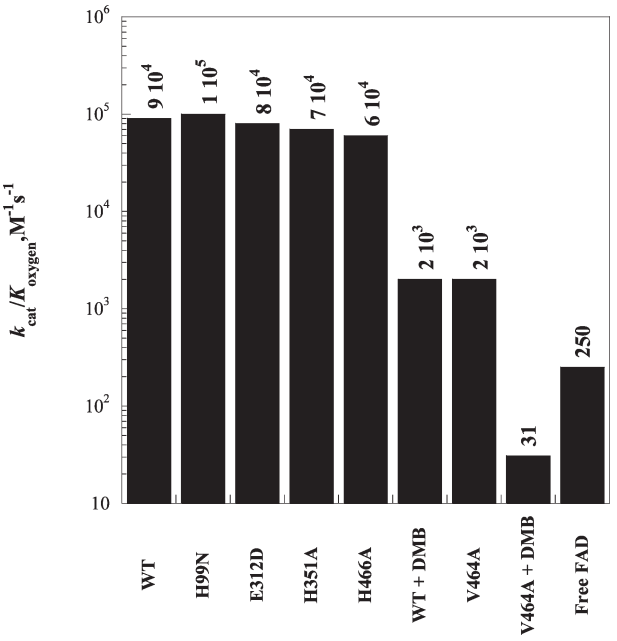


FIGURE 6: $k_{cat}/K_{oxygen}$ values for the wild-type enzyme as well as variant forms of choline oxidase with mutations in the active site at pH 10.0 and 25 °C with the exception of WT + DMB and V464A + DMB which are at pH 8.0 and 25 °C. As a reference the rate of oxidation of free flavin by oxygen at pH 6.5 is added. Data are from this study and refs *1*, *15*, *16*, (*25*−*27*,) and *38*.

~55-fold was previously reported for the wild-type enzyme with the substrate devoid of positive charge (i.e., 90000 $M^{-1}$ $s^{-1}$ and 1600 $M^{-1}$ $s^{-1}$ with choline and 3,3-dimethylbutan-1-ol, respectively) (*15*, *16*). In contrast, the $k_{cat}/K_{oxygen}$ values for a number of active site variants of choline oxidase with point mutations of residues shown to be important for catalysis either in direct contact with or further removed from Val464 (i.e., His99Asn, Gly312Asp, His351Ala, and His466Ala) were shown previously not to be significantly different from the wild-type, as summarized in Figure 6 (*1*, *15*, *25*−*27*, *38*).

## DISCUSSION

In this study, the role of Val464 in the reaction of flavin oxidation catalyzed by choline oxidase was investigated with site-directed mutagenesis, steady-state and rapid kinetics, and X-ray crystallography. Val464, which sits in the active site of the enzyme on the *re*-face at ~5.0 Å from the C(4a) and the N(5) atoms of the flavin, was replaced with alanine or threonine, and the effects of the mutations on the properties of the enzyme were investigated. The overall three-dimensional structure, as well as the location and conformation of all the active site residues in the Val464Ala enzyme, was shown by X-ray crystallography to be essentially identical to that of the wild-type enzyme (*25*). Consistent with an unaltered enzyme structure, a number of functional properties were shared by the mutant and wild-type enzymes, as demonstrated in this and a previous study (*28*). The Val464Ala and the wild-type enzymes catalyze the oxidation of choline through a sequential steady-state kinetic mechanism, consistent with a similar order of substrate binding and product release during turnover. In addition, the Val464Ala enzyme shows a pH-independent $k_{cat}/K_{oxygen}$ value with choline and a significantly lower $k_{cat}/K_{oxygen}$ value with 3,3-dimethylbutan-1-ol with respect to choline as substrate, as does the wild-type enzyme. Finally, a recent study showed that the competent forms of Ala464 and

Thr464 variants of choline oxidase contain covalently bound FAD, stabilize an anionic flavosemiquinone in the presence of air, have UV−visible absorbance spectra with no sign of protein denaturation, and kinetic isotope effects on the $k_{red}$ values at pH 10.0 that are within 3-fold from the values of the wild-type enzyme (*28*). These structural and functional observations unequivocally establish that the role of Val464 in the reaction of flavin oxidation catalyzed by choline oxidase can be elucidated by comparing and contrasting the mechanistic properties of the Val464Ala and Val464Thr enzymes with those of the wild-type enzyme.

The active site residue Val464 is important for the oxidation of the reduced flavin by molecular oxygen but not for substrate binding or the hydride ion transfer reaction that occurs between the choline substrate and the flavin cofactor. Evidence in support of this conclusion comes from the comparison of the kinetic data of the Val464Ala and Val464Thr enzymes with those for the wild-type form of choline oxidase. In summary, replacement of Val464 with alanine or threonine results in a 2-fold decrease in the limiting rate constant for flavin reduction ($k_{red}$) and less than 5-fold decrease in the equilibrium constant for formation of the enzyme−substrate complex ($K_d$) (*28*). In the Val464Ala variant enzyme the substitution of the valine with an alanine results in a 50-fold decrease in the bimolecular rate constant for reaction with oxygen, $k_{cat}/K_{oxygen}$. In the Val464Thr variant enzyme a direct measurement of the $k_{cat}/K_{oxygen}$ values could not be carried out due to the inability to saturate the enzyme with oxygen and the sigmoidal kinetic patterns of the initial rates of reaction as a function of oxygen concentration. However, the similar kinetic behavior of the Val464Thr and Val464Ala enzymes in enzyme-monitored turnover experiments, along with the rate of oxidation of the free form of enzyme and reduction being similar for the two enzymes, is consistent with them having similar overall rates for flavin oxidation. At pH 10.0, an in-depth mechanistic investigation of the reductive half-reaction of the mutant enzymes using solvent and substrate kinetic isotope effects previously established that the replacement of Val464 with alanine or threonine significantly slows down the cleavage of the OH bond of choline but has a minimal effect on the rate of hydride ion transfer that is associated with the cleavage of the CH bond of choline (*28*).

We propose that the role of Val464 in the oxidation reaction where the reduced flavin reacts with oxygen is to provide a nonpolar site proximal to the C(4a) atom of the flavin in order to guide oxygen at the site where the presence of the nearby positively charged catalyst will subsequently activate it to the superoxide species. Evidence for this conclusion comes from the effect on the bimolecular rate constant for reaction of the reduced flavin with oxygen upon replacing Val464 with alanine, which results in a 50-fold decrease in the $k_{cat}/K_{oxygen}$ value. As shown by the comparison of the crystallographic structures of the mutant and the wild-type enzyme, such an amino acid substitution increases the size of the cavity on the *re*-face of the flavin that is proximal to the C(4a)-N(5) atoms, where the C(4a) oxygen adduct is observed in the wild-type enzyme, but produces no other observable changes in the structure of the active site. Evidence for the importance of a nonpolar site in proximity of the C(4a) atom of the flavin comes from the similar effect on the oxidative half-reaction that is seen in the enzymes containing alanine or threonine at residue 464. Additionally, no significant effects on $k_{cat}/K_{oxygen}$ are observed upon mutating the remaining residues (His351 and His466) that define the cavity on the *re*-face directly above the C(4a)-N(5) atoms of the flavin or any of the other active site residues that have been shown to participate in catalysis (*27*, *38*).

The requirement in choline oxidase for a nonpolar site in proximity of the C(4a) atom of the flavin is not associated with the presence of the electrostatic catalyst that will subsequently activate oxygen for the reaction with the flavin. In this regard, previous studies established that the positive charge that is required to activate oxygen in choline oxidase is provided by the trimethylammonium group of the enzyme-bound substrate and not by a side chain of an amino acid in the active site of the enzyme (*15*, *27*, *37*, *38*). Evidence for the effect of the nonpolar site being independent of the charge that activates oxygen comes from the comparison of the $k_{cat}/K_{oxygen}$ values of the wild-type and Val464Ala enzymes determined with choline and 3,3-dimethylbutan-1-ol as substrate. Replacement of Val464 with alanine results in a $\Delta\Delta G$ of 2.3 ± 0.2 kcal mol$^{-1}$ as calculated from the ratio of the $k_{cat}/K_{oxygen}$ values determined with choline as substrate for the wild-type and Val464Ala enzymes. Analogously, a $\Delta\Delta G$ of 2.4 ± 0.2 kcal mol$^{-1}$ can be estimated for the wild-type enzyme upon taking the ratio of the $k_{cat}/K_{oxygen}$ values determined with 3,3-dimethylbutan-1-ol and choline. These values define the individual energetic contributions of the residue at position 464 and the charge harbored on the substrate toward the reaction of the reduced flavin with oxygen. When both contributions are taken into account, by taking the ratio of the $k_{cat}/K_{oxygen}$ values determined with choline as substrate for the wild-type enzyme and 3,3-dimethylbutan-1-ol as substrate for the Val464Ala enzyme, a $\Delta\Delta G$ of 4.7 ± 0.5 kcal mol$^{-1}$ can be estimated. This experimental value agrees well with the sum of the individual contributions (i.e., 4.7 ± 0.6 kcal mol$^{-1}$), consistent with the two effects being additive and independent of one another (*51*).

Analysis of a number of flavoprotein oxidases whose three-dimensional structure is known suggests that a nonpolar site of the type identified in this study in choline oxidase is likely a general feature in the class of enzymes. Here, we will limit our discussion to the cases of glucose oxidase and monomeric sarcosine oxidase, for which experimental evidence for activation of oxygen by a positive charge has been previously provided (*11*−*14*). In the three-dimensional structure of glucose oxidase, Val560 is ~4.7 Å away from the side chain of His516, which provides the positive charge for oxygen activation (*11*−*13*), and less than 6.5 Å from the C(4a) atom of the flavin. Similarly, in the active site of monomeric sarcosine oxidase Phe256 is less than 4 Å away from the side chain of Lys265, which has been shown to activate oxygen for reaction with the reduced flavin with its positive charge (*14*), and less than 6 Å from the C(4a) atom of the flavin. A possible rationale for why these sites in oxidases are not as immediately evident from the structure as in the case of the monooxygenase component $C_2$ of *p*-hydroxyphenylacetate hydroxylase (*19*), but require a mechanistic investigation of the enzymes, is likely that in oxidases the requirement of a nonpolar cavity that encapsulates and stabilizes crucial reaction intermediates is not as stringent as in monooxygenases. Monooxygenases are required to completely desolvate the cavity surrounding the C(4a) atom of the flavin to allow longer lifetimes for reaction intermediates such as C(4a)-(hydro)peroxides and C(4a)-hydroxides (*19*). Most likely oxidases do not share this requirement, either because oxygen reduction occurs through outer-sphere electron transfers without formation of any C(4a)-flavin adduct with the flavin (*10*) or simply because once oxygen is activated for reaction there is no need to prolong the lifetime of C(4a)-flavin

adduct intermediates that will decay to hydrogen peroxide without being used to hydroxylate organic substrates.

In conclusion the results of the mechanistic and structural investigation of active site mutant enzymes where the hydrophobic residue Val464 is replaced with either alanine or threonine are consistent with the presence of a nonpolar site in proximity of the C(4a)-N(5) atoms of the flavin being required for catalysis in choline oxidase. The presence of such a nonpolar site is important for the oxidative half-reaction in which the enzyme-bound reduced flavin reacts with molecular oxygen to produce hydrogen peroxide and complete the catalytic cycle. It is proposed that the function of the nonpolar, aminoacyl side chain is to guide oxygen at the site where it subsequently will be activated to a superoxide species through electrostatic catalysis exerted by a positive charge. The results also suggest that these two events in the reaction with oxygen catalyzed by choline oxidase are independent of one another. It is expected that nonpolar sites of the kind identified in this study in choline oxidase will be identified through mechanistic investigation in a number of flavoprotein oxidases with various overall folding topologies including PHBH folds and $(\alpha/\beta)_8$ barrels, as suggested from visual surveys of available crystal structures of flavin-dependent oxidases, such as old yellow enzyme, glycolate oxidase, cholesterol oxidase, and vanillyl-alcohol oxidase.

## ACKNOWLEDGMENT

The authors thank Jane V. Hoang for the site-directed mutagenesis to prepare the Val464Ala enzyme and for the pH profile of the $k_{cat}/K_{oxygen}$ values and Andrea Pennati for help in the site-directed mutagenesis of the Val464Leu enzyme. We thank the staff at the SER-CAT beamlines at the Advanced Photon Source, Argonne National Laboratory, for assistance during X-ray data collection. Use of the Advanced Photon Source was supported by the U.S. Department of Energy, Basic Energy Sciences, Office of Science, under Contract W-31-109-Eng-38.

## REFERENCES

1. Massey, V. (1994) Activation of molecular oxygen by flavins and flavoproteins. *J. Biol. Chem. 269*, 22459–22462.
2. Mattevi, A. (2006) To be or not to be an oxidase: challenging the oxygen reactivity of flavoenzymes. *Trends Biochem. Sci. 31*, 276–283.
3. Kemal, C., and Bruice, T. C. (1976) Simple synthesis of a 4a-hydroperoxy adduct of a 1,5-dihydroflavine: preliminary studies of a model for bacterial luciferase. *Proc. Natl. Acad. Sci. U.S.A. 73*, 995–999.
4. Massey, V. (2000) The chemical and biological versatility of riboflavin. *Biochem. Soc. Trans. 28*, 283–296.
5. Ghisla, S., and Massey, V. (1989) Mechanisms of flavoprotein-catalyzed reactions. *Eur. J. Biochem. 181*, 1–17.
6. Wang, R., and Thorpe, C. (1991) Reactivity of medium-chain acyl-CoA dehydrogenase toward molecular oxygen. *Biochemistry 30*, 7895–7901.
7. DuPlessis, E. R., Pellett, J., Stankovich, M. T., and Thorpe, C. (1998) Oxidase activity of the acyl-CoA dehydrogenases. *Biochemistry 37*, 10469–10477.
8. Sun, W., Williams, C. H., Jr., and Massey, V. (1996) Site-directed mutagenesis of glycine 99 to alanine in L-lactate monooxygenase from *Mycobacterium smegmatis*. *J. Biol. Chem. 271*, 17226–17233.
9. Leferink, N. G., Fraaije, M. W., Joosten, H. J., Schaap, P. J., Mattevi, A., and van Berkel, W. J. (2009) Identification of a gatekeeper residue that prevents dehydrogenases from acting as oxidases. *J. Biol. Chem. 284*, 4392–4397.
10. Klinman, J. P. (2007) How do enzymes activate oxygen without inactivating themselves? *Acc. Chem. Res. 40*, 325–333.
11. Roth, J. P., Wincek, R., Nodet, G., Edmondson, D. E., McIntire, W. S., and Klinman, J. P. (2004) Oxygen isotope effects on electron transfer to O2 probed using chemically modified flavins bound to glucose oxidase. *J. Am. Chem. Soc. 126*, 15120–15131.
12. Roth, J. P., and Klinman, J. P. (2003) Catalysis of electron transfer during activation of O2 by the flavoprotein glucose oxidase. *Proc. Natl. Acad. Sci. U.S.A. 100*, 62–67.
13. Su, Q., and Klinman, J. P. (1999) Nature of oxygen activation in glucose oxidase from *Aspergillus niger*: the importance of electrostatic stabilization in superoxide formation. *Biochemistry 38*, 8572–8581.
14. Zhao, G., Bruckner, R. C., and Jorns, M. S. (2008) Identification of the oxygen activation site in monomeric sarcosine oxidase: role of Lys265 in catalysis. *Biochemistry 47*, 9124–9135.
15. Gadda, G., Fan, F., and Hoang, J. V. (2006) On the contribution of the positively charged headgroup of choline to substrate binding and catalysis in the reaction catalyzed by choline oxidase. *Arch. Biochem. Biophys. 451*, 182–187.
16. Gadda, G., Powell, N. L., and Menon, P. (2004) The trimethylammonium headgroup of choline is a major determinant for substrate binding and specificity in choline oxidase. *Arch. Biochem. Biophys. 430*, 264–273.
17. Chen, L., Lyubimov, A. Y., Brammer, L., Vrielink, A., and Sampson, N. S. (2008) The binding and release of oxygen and hydrogen peroxide are directed by a hydrophobic tunnel in cholesterol oxidase. *Biochemistry 47*, 5368–5377.
18. Baron, R., Riley, C., Chenprakhon, P., Thotsaporn, K., Winter, R. T., Alfieri, A., Forneris, F., van Berkel, W. J., Chaiyen, P., Fraaije, M. W., Mattevi, A., and McCammon, J. A. (2009) Multiple pathways guide oxygen diffusion into flavoenzyme active sites. *Proc. Natl. Acad. Sci. U.S.A. 106*, 10603–10608.
19. Alfieri, A., Fersini, F., Ruangchan, N., Prongjit, M., Chaiyen, P., and Mattevi, A. (2007) Structure of the monooxygenase component of a two-component flavoprotein monooxygenase. *Proc. Natl. Acad. Sci. U.S.A. 104*, 1177–1182.
20. Hoang, J. V., and Gadda, G. (2007) Trapping choline oxidase in a nonfunctional conformation by freezing at low pH. *Proteins 66*, 611–620.
21. Ghanem, M., and Gadda, G. (2006) Effects of reversing the protein positive charge in the proximity of the flavin N(1) locus of choline oxidase. *Biochemistry 45*, 3437–3447.
22. Fan, F., Ghanem, M., and Gadda, G. (2004) Cloning, sequence analysis, and purification of choline oxidase from *Arthrobacter globiformis*: a bacterial enzyme involved in osmotic stress tolerance. *Arch. Biochem. Biophys. 421*, 149–158.
23. Ghanem, M., Fan, F., Francis, K., and Gadda, G. (2003) Spectroscopic and kinetic properties of recombinant choline oxidase from *Arthrobacter globiformis*. *Biochemistry 42*, 15179–15188.
24. Orville, A. M., Lountos, G. T., Finnegan, S., Gadda, G., and Prabhakar, R. (2009) Crystallographic, spectroscopic, and computational analysis of a flavin C4a-oxygen adduct in choline oxidase. *Biochemistry 48*, 720–728.
25. Quaye, O., Lountos, G. T., Fan, F., Orville, A. M., and Gadda, G. (2008) Role of Glu312 in binding and positioning of the substrate for the hydride transfer reaction in choline oxidase. *Biochemistry 47*, 243–256.
26. Gadda, G., Quaye, O., Cowins, S. (2009) Contribution of flavin covalent linkage with histidine 99 to the reaction catalyzed by choline oxidase, J. Biol. Chem. (in press).
27. Rungsrisuriyachai, K., and Gadda, G. (2008) On the role of histidine 351 in the reaction of alcohol oxidation catalyzed by choline oxidase. *Biochemistry 47*, 6762–6769.
28. Finnegan, S., and Gadda, G. (2008) Substitution of an active site valine uncovers a kinetically slow equilibrium between competent and incompetent forms of choline oxidase. *Biochemistry 47*, 13850–13861.
29. Fan, F., and Gadda, G. (2007) An internal equilibrium preorganizes the enzyme-substrate complex for hydride tunneling in choline oxidase. *Biochemistry 46*, 6402–6408.
30. Fan, F., Germann, M. W., and Gadda, G. (2006) Mechanistic studies of choline oxidase with betaine aldehyde and its isosteric analogue 3,3-dimethylbutyraldehyde. *Biochemistry 45*, 1979–1986.
31. Fan, F., and Gadda, G. (2005) Oxygen- and temperature-dependent kinetic isotope effects in choline oxidase: correlating reversible hydride transfer with environmentally enhanced tunneling. *J. Am. Chem. Soc. 127*, 17954–17961.
32. Fan, F., and Gadda, G. (2005) On the catalytic mechanism of choline oxidase. *J. Am. Chem. Soc. 127*, 2067–2074.
33. Gadda, G. (2003) pH and deuterium kinetic isotope effects studies on the oxidation of choline to betaine-aldehyde catalyzed by choline oxidase. *Biochim. Biophys. Acta 1650*, 4–9.
34. Gadda, G. (2003) Kinetic mechanism of choline oxidase from *Arthrobacter globiformis*. *Biochim. Biophys. Acta 1646*, 112–118.
35. Quaye, O., and Gadda, G. (2009) Effect of a conservative mutation of an active site residue involved in substrate binding on the hydride

tunneling reaction catalyzed by choline oxidase. *Arch. Biochem. Biophys. 489*, 10–14.
36. Gadda, G. (2008) Hydride transfer made easy in the reaction of alcohol oxidation catalyzed by flavin-dependent oxidases. *Biochemistry 47*, 13745–13753.
37. Quaye, O., Cowins, S., and Gadda, G. (2009) Contribution of flavin covalent linkage with histidine 99 to the reaction catalyzed by choline oxidase. *J. Biol. Chem. 284*, 16990–16997.
38. Ghanem, M., and Gadda, G. (2005) On the catalytic role of the conserved active site residue His466 of choline oxidase. *Biochemistry 44*, 893–904.
39. Minor, Z. O. A. W. (1997) Processing of X-ray diffraction data collected in oscillation mode. *Methods Enzymol. 276*, 307–326.
40. McCoy, A. J., Grosse-Kunstleve, R. W., Storoni, L. C., and Read, R. J. (2005) Likelihood-enhanced fast translation functions. *Acta Crystallogr., Sect. D: Biol. Crystallogr. 61*, 458–464.
41. Murshudov, G. N., Vagin, A. A., and Dodson, E. J. (1997) Refinement of macromolecular structures by the maximum-likelihood method. *Acta Crystallogr., Sect. D: Biol. Crystallogr. 53*, 240–255.
42. Jones, T. A., Zou, J. Y., Cowan, S. W., and Kjeldgaard, M. (1991) Improved methods for building protein models in electron density maps and the location of errors in these models. *Acta Crystallogr. A 47* (Part 2), 110–119.
43. Emsley, P., and Cowtan, K. (2004) Coot: model-building tools for molecular graphics. *Acta Crystallogr., Sect. D: Biol. Crystallogr. 60*, 2126–2132.
44. Lovell, S. C., Davis, I. W., Arendall, W. B., III, de Bakker, P. I., Word, J. M., Prisant, M. G., Richardson, J. S., and Richardson, D. C. (2003) Structure validation by Calpha geometry: phi,psi and Cbeta deviation. *Proteins 50*, 437–450.
45. Merritt, E. A., and Murphy, M. E. (1994) Raster3D Version 2.0. A program for photorealistic molecular graphics. *Acta Crystallogr., Sect. D: Biol. Crystallogr. 50*, 869–873.
46. Allison, D. R., and Purich, D. L. (1979) Practical considerations in the design of initial velocity enzyme rate assays, in Methods in Enzymology (Purich, D. L., Ed.) pp 3−19, Academic Press, New York.
47. Cook, P. F., and Cleland, W. W. (2007) Enzyme kinetics and mechanism, Garland Science, London and New York.
48. Fan, F., and Gadda, G. (2005) On the catalytic mechanism of choline oxidase. *J. Am. Chem. Soc. 127*, 2067–2074.
49. Ghanem, M., Fan, F., Francis, K., and Gadda, G. (2003) Spectroscopic and kinetic properties of recombinant choline oxidase from *Arthrobacter globiformis*. *Biochemistry 42*, 15179–15188.
50. Gadda, G. (2003) Kinetic mechanism of choline oxidase from *Arthrobacter globiformis*. *Biochim. Biophys. Acta 1646*, 112–118.
51. Mildvan, A. S. (2004) Inverse thinking about double mutants of enzymes. *Biochemistry 43*, 14517–14520.